Available online at www.sciencedirect.com
ScienceDirect
Journal of Molecular Structure 797 (2006) 154–164
Journal of MOLECULAR STRUCTURE
www.elsevier.com/locate/molstruc

Solid state and solution characterization of a new dinuclear nickel (II) complex: The search for synthetic models for urease

Adolfo Horn Jr. [a], Luciana Fim [a], Adailton J. Bortoluzzi [b], Bruno Szpoganicz [b], Marlon de S. Silva [b], Miguel A. Novak [c], Mario Benassi Neto [d], Lívia Schiavinato Eberlin [d], Rodrigo Ramos Catharino [d], Marcos Nogueira Eberlin [d], Christiane Fernandes [a,*]

[a] *Laboratório de Ciências Químicas, Universidade Estadual do Norte Fluminense, 28013-602 Campos dos Goytacazes, RJ, Brazil*
[b] *Departamento de Química, Universidade Federal de Santa Catarina, 88040-900 Florianópolis, SC, Brazil*
[c] *Instituto de Física, Universidade Federal do Rio de Janeiro, 21941-972 Rio de Janeiro, RJ, Brazil*
[d] *Laboratório Thomson de Espectrometria de Massas, Instituto de Química, Universidade Estadual de Campinas, 13084-971 Campinas, SP, Brazil*

Received 9 December 2005, received in revised form 10 March 2006; accepted 13 March 2006
Available online 6 May 2006

Abstract

The X-ray molecular structure and, magnetic, and spectroscopic properties, as well as the analysis of the structural behavior in solution of a novel nickel (II) complex $[Ni_2(HBPClNOL)_2(OAc)](ClO_4)$ **1** are reported. Complex **1** was prepared by the reaction between the ligand $H_2BPClNOL$ (*N*-(2-hydroxybenzyl)-*N*-(2-pyridylmethyl)[(3-chloro)(2-hydroxy)]propylamine), $[Ni(H_2O)_6](ClO_4)_2$ and sodium acetate. Magnetic measurements indicate the presence of a weak antiferromagnetic coupling between the Ni(II) ions in **1**, resulting in $J = -4.23\ cm^{-1}$. Mass spectrometric characterization of the complex **1** was also performed via ESI-MS and ESI-MS/MS experiments and reveals that there are at least three different cations in solution, one mononuclear $[Ni(H_2BPClNOL)(OAc)]^+$ and two dinuclear $[Ni_2(HBPClNOL)_2(OAc)]^+$ and $[Ni_2(HBPClNOL)_2(ClO_4)]^+$ cations, as well as likely a fourth one $[Ni(HBPClNOL)]^+$. Potentiometric titration experiments confirm that under acid conditions, the dinuclear unit is broken. However, under neutral/basic pH values the dinuclear unit is stable and shows the presence of two water molecules coordinated to the nickel ions, resulting in the cation $[Ni_2(HBPClNOL)_2(H_2O)_2]^{2+}$. This cation shows two protonation/deprotonation equilibriums with pK_a values of 9.68 and at 10.29, which are related to the aquo/hydroxo equilibrium associated with the water molecules coordinated to the metal ions.

Keywords: Urease; Dinuclear nickel (II) complex; X-ray; Potentiometric studies; ESI-MS/MS

1. Introduction

Urease (urea amidohydrolase EC 3.5.1.5) is a nickel-dependent metalloenzyme that catalyses the hydrolysis of urea to ammonia and carbon dioxide, in conjunction with biological functions using urea as a nitrogen source [1,2]. It was the first metalloenzyme crystallized from jack beans by James Summer in 1926, and is the only metallohydrolase that utilizes nickel [3]. In 1995, an X-ray molecular structure of *Klebsiella aerogenes* urease with a resolution of 2.2 Å was reported [4]. The two nickel ions are bridged by a carboxylate group of a carbamylated lysine residue with a Ni···Ni separation of 3.5 Å. The geometrical structure around one nickel (Ni1) ion is pseudo-tetrahedral with two histidine nitrogen atoms, an oxygen atom of the carbamate bridge, and a water molecule; the fourth position is only partially occupied by a water molecule and considered to be a likely candidate for binding urea during the catalysis process. The geometry around the second nickel (Ni2) is depicted as trigonal bipyramidal with further coordination of an asparagine oxygen.

In 1989, Clark and Wilkox, from magnetic susceptibility data of jack bean urease, reported the existence of a weak antiferromagnetic exchange coupling between two nickel

* Corresponding author. Tel.: +55 22 2526 1494; fax: +55 22 2526 1519.
E-mail address: chrisf@uenf.br (C. Fernandes).

0022-2860/$ - see front matter © 2006 Elsevier B.V. All rights reserved.
doi:10.1016/j.molstruc.2006.03.043

(II) ions, resulting in $2J = -12.6\ cm^{-1}$ [5]. Day and co-workers have, however, pointed out that the two nickel (II) ions are magnetically non-coupled in the active site of urease [6]. In addition, variable-temperature MCD studies have detected a ferromagnetically coupled dinuclear nickel (II) [7].

Urease converts urea to products at a rate of least 10^{14} times faster than the urea spontaneous decomposition rate [8]. The proposed mechanism of urea hydrolysis at the active site of the enzyme involves: (i) production of a hydroxide ion at the dinickel (II) center; (ii) activation of the substrate by coordination to one or both metal ions, and (iii) nucleophilic attack of the hydroxide ion at the carbonyl carbon atom of the substrate, producing ammonia and carbamic acid, which spontaneously decompose, at physiological pH, to give a second molecule of ammonia and bicarbonate [9]. Both nickel ions are involved in the catalytic reaction. Karplus and Hausinger have suggested a coordination of the carbonyl oxygen atom of urea to Ni(1) followed by a nucleophilic attack of a hydroxide ion coordinated to Ni(2). In contrast, Ciurli and co-workers have proposed that urea bridges the two metal ions via its carbonyl oxygen atom and the NH_2 group of the urea. They suggest that a nucleophilic attack may occur via a bridging hydroxide ion [10,11].

There have been a number of reports of the syntheses of dinuclear nickel complexes to model the active site of urease and several of these have a urea molecule bound to the nickel center through its carbonyl oxygen atom and this coordination mode is likely to occur in the enzyme [12].

In the search for synthetic models for metallohydrolases, we synthesized a new binuclear nickel compound $[Ni_2(HBPClNOL)_2(OAc)](ClO_4)$ **1** and report herein its physicochemical and structural properties. Potentiometric titration experiments carried out in ethanol/water solution reveal that water molecules are coordinated to the dinuclear unit by the displacement of the acetate bridge, under alkaline pH conditions. This feature has been considered essential for the hydrolytic activity of a number of metallohydrolases, including urease.

We have previously described the coordination chemistry of the ligand $H_2BPClNOL$ with iron ions; this ligand was used to obtain synthetic models for the active site of purple acid phosphatase, a dinuclear iron hydrolase [13]. To our surprise, the ligand $H_2BPClNOL$ exhibited a different coordination mode with nickel ions, revealing that the coordination mode of this ligand $H_2BPClNOL$ is dependent on the Lewis acidity of the metal center.

2. Experimental

2.1. Materials, instrumentation and general procedures

All reagents and solvents for syntheses and analyses were of analytical and/or spectroscopic grade and used without further purification. Elemental (C, H, N) analysis was performed on a Perkin-Elmer 2400 CHN analyzer. Infrared spectra were recorded in KBr pellets on a Nicolet-Magna IR 760 instrument and the electronic absorption spectra (200–1000 nm range) were recorded in acetonitrile with a Shimadzu 1601 PC UV–Vis spectrophotometer. Conductivity of **1** was measured at room temperature using a Biocristal conductometer.

Low temperature Isothermal Magnetization and temperature dependence of the Magnetic Susceptibility measurements were made on a crystalline sample of **1** in the temperature range of 2–300 K in an applied field of $H < 9$ T using a Quantum Design PPMS magnetometer. The diamagnetism of the sample and sample holder was taken into account by subtracting an estimated temperature independent term.

The potentiometric studies were carried out with a Corning 350 digital pH meter fitted with blue-glass and Ag/AgCl reference electrodes calibrated to read $-\log[H^+]$ directly, designated as pH. Bidistilled water in the presence of $KMnO_4$ was used to prepare the ethanol/water 70/30% v/v ($pK_w = 14.78$) solutions. The electrode was calibrated using the data obtained from the potentiometric titration of a known volume of a standard 0.100 M HCl solution with a standard 0.100 M KOH solution, both in an ethanol/water 70/30 % v/v solution. The ionic strength of the HCl solution was maintained at 0.100 M by addition of KCl. The measurements were carried out in a thermostated cell containing a complex solution (0.05 mol/50 mL) with ionic strength adjusted to 0.100 M by addition of KCl, at 25.00 ± 0.050 °C. The experiments were performed under argon flow to eliminate the presence of atmospheric CO_2. The samples were titrated by addition of fixed volumes of a standard CO_2-free KOH solution (0.100 M). Computations were carried out with the BEST7 program, and species distribution diagrams were obtained with SPE and SPEPLOT programs [14].

The mass spectrometry (MS) experiments were carried out using a Q-TOF mass spectrometer (Micromass, Manchester, UK). The ionization technique used was electrospray ionization in the positive mode (ESI (+)-MS). Typical MS conditions were: source temperature of 80 °C, dessolvation temperature of 80 °C, capillary voltage of 3 kV and cone voltage of 40 V. Complex **1** was diluted in methanol and water (1:1) in a 1 mL flask. While the quality of the ESI-MS/MS spectrum is better in methanol/water (1:1) than in ethanol/water, the latter is more suitable for potentiometric studies. The sample was injected using a syringe pump (Harvard Apparatus) at a flow rate of $10\ \mu L\ min^{-1}$. Mass spectra were acquired along the 50–1500 m/z range. ESI-MS/MS was performed by mass-selecting the ion of interest using the first quadrupole Q1. The selected ion was in turn subjected to 5–30 eV collisions with argon in the second rf-only collision quadrupole (Q2) while scanning the orthogonal TOF mass analyzer to acquire its tandem mass spectrum. The collision gas pressure was optimized to produce extensive dissociation with minimal loss of ion current.

2.2. Syntheses

2.2.1. N-(2-hydroxybenzyl)-N-(2-pyridylmethyl)-[(3-chloro)(2-hydroxy)] propylamine ($H_2BPClNOL$)

The ligand $H_2BPClNOL$ was prepared through the reaction between *N*-(2-hydroxybenzyl)-*N*-(2-pyridylmethyl)amine (HBPA) [15] and an equimolar amount of epichlorohydrin as has been reported previously [16].

2.2.2. Synthesis of the complex $[Ni_2(HBPClNOL)_2(OAc)](ClO_4)$ **1**

Caution. No problems were encountered during the preparation of the perchlorate derivative described above. However, suitable care must be taken when handling such potentially explosive materials.

A methanolic solution of $[Ni(OH_2)_6](ClO_4)_2$ (365 mg, 1 mmol) was added to a methanolic solution (15 mL) of the ligand $H_2BPClNOL$ (307 mg, 1 mmol), resulting in a green solution. To this mixture, dehydrated NaOAc (495 mg, 6 mmol) was added, resulting in a deep green solution. The reaction mixture was then stirred for 30 min and allowed to stand at room temperature for one week. Blue single crystals were formed, filtered off and washed with methanol. Yield: 33%. Anal. Found: C, 46.03; H, 4.45; N, 6.33. Calcd for $Ni_2C_{34}H_{39}N_4O_{10}Cl_3$: C, 46.01; H, 4.43; N, 6.31%. IR (KBr pellet, cm^{-1}): 3374, 3065, 3032, 2963, 2923, 1596, 1580, 1455, 1433, 1309, 1132, 760. Λ_M(acetonitrile) = 160 $cm^2\,\Omega^{-1}\,mol^{-1}$ (1:1 electrolyte type) [17].

2.3. Crystallographic data collection and structure determination

The crystal data were obtained on an Enraf-Nonius CAD4 diffractometer, using graphite monochromated Mo-K_α radiation ($\lambda = 0.71069$ Å), at room temperature. A blue crystal was isolated from a homogeneous crystalline sample of **1**. Unit-cell parameters were determined by centering 25 reflections in the θ range 8.45–14.98° and refined by the least-squares method. Intensities were collected using the $\omega - 2\theta$ scan technique. Three standard reflections were monitored every 200 reflections throughout the data collection and no significant intensity decay was observed. All diffracted intensities were corrected for Lorentz and polarization effects [18]. Empirical absorption correction based on the azimuthal scans of seven appropriate reflections was also applied to the collected intensities using the PLATON program [19]. The structure was solved by direct methods and was refined by the full-matrix least-squares method using SIR97 [20] and SHELXL97 [21] computer programs, respectively. All non-hydrogen atoms were refined with anisotropic displacement parameters. The oxygen atoms of the perchlorate counterion were found disordered over two alternative positions. These atoms were refined anisotropically with 0.56(3) and 0.44(3) site occupancies. For the best results in the modeling process, 73 thermal and 64 positional restraints were applied to the disordered group. The hydrogen atom of the alcohol was found from the Fourier map, whereas all other H atoms were placed at idealized positions using standard geometric criteria. The ORTEP-3 [22] program was used to generate the diagram of the molecular structure. Further relevant crystallographic data are summarized in Table 1.

Table 1
Crystal data and structure refinement for complex **1**

Empirical formula	$C_{34}H_{39}Cl_3N_4Ni_2O_{10}$
Formula weight	887.46
Temperature (K)	293(2)
Wavelength (Å)	0.71069
Crystal system	Orthorhombic
Space group	$Pna2_1$
a (Å)	18.798(1)
b (Å)	19.705(2)
c (Å)	10.270(2)
Volume (Å^3)	3804.2(9)
Z	4
ρ_{calc} (g/cm^3)	1.550
μ (mm^{-1})	1.261
F (000)	1832
Crystal size	0.46 × 0.30 × 0.30 mm
Theta range for data collection	1.50–28.75°
Index ranges	$-25 \leqslant h \leqslant 0$, $-26 \leqslant k \leqslant 0$, $-13 \leqslant l \leqslant 0$
Reflections collected/unique	5195/5195
Absorption correction	Psi-scan
Max. and min. transmission	0.635 and 0.683
Refinement method	Full-matrix least-squares on F^2
Data/restraints/parameters	5195/137/515
Goodness-of-fit on F^2	0.930
Final *R* indices [$I > 2\sigma(I)$]	$R_1 = 0.0429$, $wR_2 = 0.0832$
R indices (all data)	$R_1 = 0.1276$, $wR_2 = 0.0928$
Largest diff. peak and hole (e Å^{-3})	0.375 and −0.318

3. Results and discussion

3.1. Synthesis and general characterization

The synthesis of **1** was achieved through the reaction between $[Ni(H_2O)_6](ClO_4)_2$, the ligand $H_2BPClNOL$ and sodium acetate in a 1:1:6 ratio, according to the experimental conditions described in Section 2.2.2. A large excess of NaOAc was utilized in order to promote the deprotonation of the phenol groups, which act as bridging groups between the nickel centers.

The infrared spectrum of **1** displays bands assignable to a bridging acetate at 1580 and 1455 cm^{-1} ($\Delta = 125$ cm^{-1}) [23], the counter-ion ClO_4^- at 1132 cm^{-1} and typical bands of the ligand $H_2BPClNOL$.

3.2. Description and discussion of the crystal structure of complex **1**

The X-ray crystal structure of **1** reveals that the complex consists of a dinuclear nickel cation containing a perchlorate as a counter-ion. Each nickel center is coordinated

to two nitrogen (aminic and pyridinic) and four oxygen (phenolate, alcohol and acetate) atoms, resulting in the same environmental coordination for both metal centers. A perspective view of the cation is displayed in Fig. 1 and the selected bond lengths and angles are presented in Table 2. In **1**, both nickel atoms are six-coordinated in a distorted octahedral environment. The metal centers Ni1 and Ni2 are linked by two ligand-derived phenolates (O10 and O30) and by one acetate ion (O51 and O52). The aminic nitrogen atoms (N1 and N2), pyridinic nitrogen atoms (N22 and N42) and the alcohol oxygen atoms (O1 and O2) complete the N2O4 coordination sphere for Ni1 and Ni2 atoms. The Ni1···Ni2 distance is 3.0154(9) Å. The Ni1–O10–Ni2 and Ni1–O30–Ni2 bridging angles are 96.60(15)° and 96.24(15)°, respectively, which are smaller than those found for similarly coordinated μ-phenolate nickel (II) dimers. For the complex reported by Greatti and co-workers, this angle is 118.01(16)° [24] and for the complex reported by Brito and co-workers it is 131.8(1)° [25]. This difference can be justified by the presence of two phenolate bridges in **1**, while in the complexes reported by Greatti and Brito, only one phenolate bridge is present.

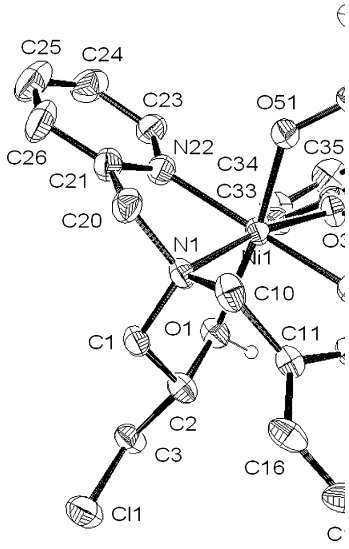

Fig. 1. View of the binuclear cation $\mathbf{1}^{+}$ with labeling scheme. The ellipsoids are shown at the 40% probability level.

Table 2
Selected bond lengths [Å] and angles [°] for complex **1**

Ni1–O30	2.017(4)	Ni2–O10	2.011(3)
Ni1–O10	2.028(3)	Ni2–O30	2.033(3)
Ni1–O51	2.034(4)	Ni2–O52	2.037(4)
Ni1–N22	2.081(5)	Ni2–N2	2.086(4)
Ni1–N1	2.096(5)	Ni2–N42	2.097(4)
Ni1–O1	2.192(4)	Ni2–O2	2.147(4)
Ni1···Ni2	3.0154(9)		
O30–Ni1–O10	79.40(14)	O10–Ni2–O52	94.72(16)
O30–Ni1–O51	93.75(16)	O30–Ni2–O52	90.67(16)
O10–Ni1–O51	91.10(15)	O10–Ni2–N2	170.02(16)
O30–Ni1–N22	107.34(17)	O30–Ni2–N2	93.55(16)
O10–Ni1–N22	171.38(17)	O52–Ni2–N2	92.43(17)
O51–Ni1–N22	83.21(16)	O10–Ni2–N42	106.67(16)
O30–Ni1–N1	170.00(17)	O30–Ni2–N42	171.96(18)
O10–Ni1–N1	92.41(15)	O52–Ni2–N42	83.68(16)
O51–Ni1–N1	92.13(15)	N2–Ni2–N42	81.03(18)
N22–Ni1–N1	81.38(18)	O10–Ni2–O2	92.45(14)
O30–Ni1–O1	94.94(15)	O30–Ni2–O2	91.96(16)
O10–Ni1–O1	91.55(15)	O52–Ni2–O2	172.71(15)
O51–Ni1–O1	171.24(15)	N2–Ni2–O2	80.63(17)
N22–Ni1–O1	93.16(16)	N42–Ni2–O2	93.00(17)
N1–Ni1–O1	79.42(15)	Ni2–O10–Ni1	96.60(15)
O10–Ni2–O30	79.43(15)	Ni1–O30–Ni2	96.24(15)

The alcohol moiety from the ligand acts as a monodentate coordinated group in **1**, remaining protonated after coordination, as indicated by the long bond lengths Ni–$O_{alcohol}$ (Ni1–O1 = 2.192(4) Å and Ni2–O2 = 2.147(4) Å). The phenolate oxygen atoms are responsible for the connection between the nickel ions, acting as bridging groups. However, for the iron compounds synthesized with the same ligand, the opposite behavior was observed. In the dinuclear iron complexes $[Fe_2(BPClNOL)_2(OAc)]^{+}$ and $[Fe_2(BPClNOL)_2(H_2O)_2]^{2+}$, previously reported, the ligand $H_2BPClNOL$ exhibits a different coordination mode from that observed in complex **1** [13]. In these iron complexes, the alcohol group is deprotonated and acts as the bridging group while the phenolate group is terminally coordinated. This distinct coordination behavior of the ligand $H_2BPClNOL$ can be attributed to the difference in the Lewis acidity of the nickel (II) and the iron (III) ions, since the nickel (II) ions are not acidic enough to promote the alcohol deprotonation, which prevents their coordination as a bridging group.

Interestingly, the crystal used to obtain the molecular structure showed only molecules formed by pure S isomer form of the ligand $H_2BPClNOL$, although a racemic mixture of the ligand was employed in the synthesis of **1**.

3.3. Electronic spectroscopy

The electronic spectrum of **1**, in acetonitrile, displays three distinct bands at 611 nm ($\varepsilon = 14.8\ dm^3\ mol^{-1}\ cm^{-1}$), at 762 nm ($\varepsilon = 7.7\ dm^3\ mol^{-1}\ cm^{-1}$) and at 934 nm ($\varepsilon = 22.1\ dm^3\ mol^{-1}.\ cm^{-1}$). Considering *Oh* symmetry for the nickel ions, the bands at 611 and 934 nm can be assigned to the spin-allowed d–d transition: $^3A_{2g} \rightarrow {}^3T_{1g}$, $^3A_{2g} \rightarrow {}^3T_{2g}$, while the band at 762 nm is assigned to the spin-forbidden transition $^3A_{2g} \rightarrow {}^1E_g$. Furthermore, complex **1** presents a strong band at 300 nm ($1.0 \times 10^4\ dm^3\ mol^{-1}\ cm^{-1}$) which is attributed to the $\pi \rightarrow \pi^*$ intraligand transition [26]. The electronic spectrum of the jack bean enzyme displays absorption bands at 407, 745 and 1060 nm, which suggest octahedrally coordinated nickel (II) ions with a donor environment that is particularly rich in oxygen [27].

Complex **1** shows UV–Vis features similar to those observed in the complexes $[Ni_2L(OAc)_2(H_2O)]ClO_4.H_2O$ **2** (HL = 2-{[bis(2-pyridylmethyl)aminomethyl]}-4-methyl-6-{[(2-pyridylmethyl)aminomethyl]}phenol) and $[Ni_2(ppepO)(C_6H_5COO)(CH_3COOH)]ClO_4.C_4H_{10}O$ **3**

(ppepOH = 1-[bis(2-pyridylmethyl)amino]-3-[(2-pyridyl)ethoxy]-2-hydroxy-propane) [28]. Complex **2** shows allowed *d–d* transitions at 616 and 978 nm and the spin-forbidden transition at 778 nm while in the complex **3** these bands are located at 649, 973 and at 770 nm, respectively.

3.4. Magnetic properties of *1*

The temperature dependence of the magnetic susceptibility for compound **1** is shown in Fig. 2, presenting a typical maximum for an antiferromagnetically coupled dimer at 7.4 K. Magnetization measurements up to 9 T at 2 K (shown in the inset of Fig. 2) show an increase in the susceptibility (dM/dH) as a function of the field with inflection near 65 kOe. Both results are in agreement with the existence of weak antiferromagnetic exchange coupling between the neighboring Ni ions as expected from the structural data.

The χT vs. T curve shown in Fig. 3 is essentially flat in most of the temperature range and the value of $\chi_M T$ is

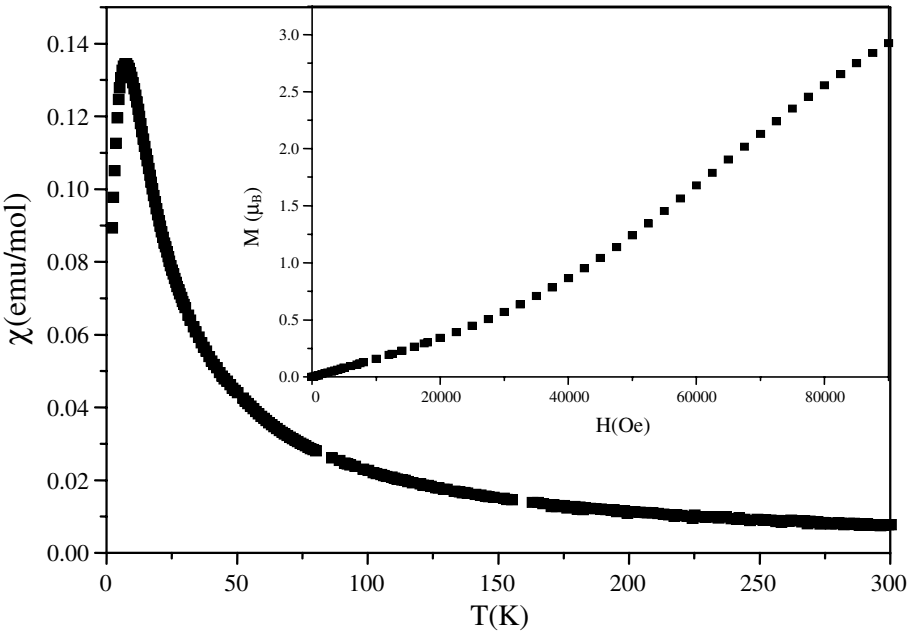

Fig. 2. Plot of χ vs. T and M vs. H at 2 K. Both have a behavior typical of an antiferromagnetic coupled dimer.

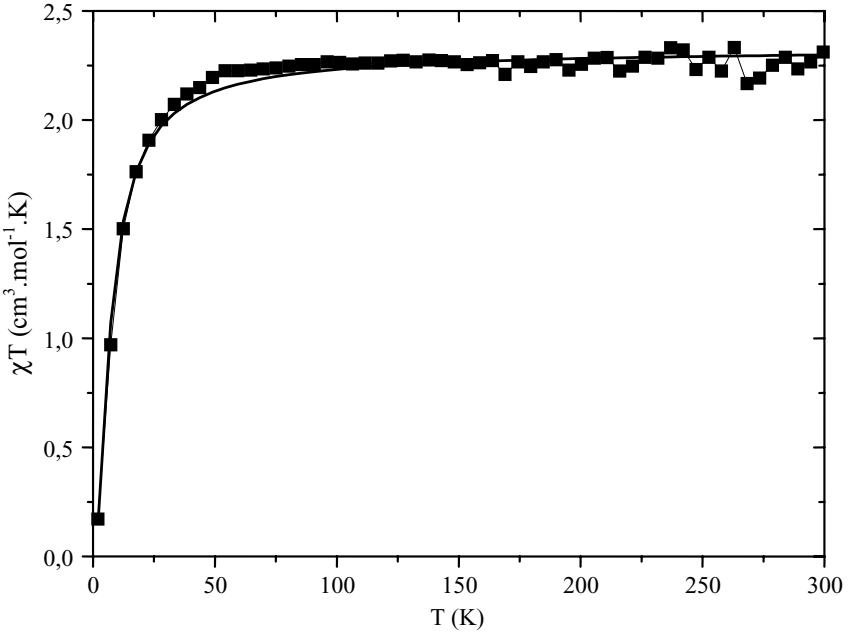

Fig. 3. Plot of χT vs. T for complex **1**. Solid line shows the best fit obtained for an AF coupled dimer.

2.27 ± 0.03 emu K/mol, giving an effective moment of 4.25 Bohr magnetons per dimer. This is near that expected for two Ni(II) isolated ions (expected value for an uncoupled nickel (II) dimer: 4.64 emu K/mol for $g = 2.159$ and $S = 1$). Below 50 K, $\chi_M T$ decreases with temperature, reaching a value of 0.26 emu K/mol at 2 K. In order to estimate the exchange interaction we used an approximate isotropic Hamiltonian $H = -2JS_1S_2$ ($S_1 = S_2 = 1$) to fit the temperature dependence of the magnetic susceptibility. A satisfactory fit, shown in Fig. 3 as a line, was obtained with $J = -4.23\ cm^{-1}$ for $g = 2.159$.

Mitra and co-workers have reported the magnetic behavior of nickel (II) complexes bridged by discrete polyatomic bridging groups (NCO, NCS, N_3, NCSe) and by a phenolate bridge. They have suggested that the phenolate group exerts an antiferromagnetic contribution [29]. The dinuclear complex $[Ni_2(\mu\text{-}OAc)_2(BIMP)]^+$, where BIMP is the ligand 2,6-bis[(bis(2-methylimidazo-2-yl)methyl)]-4-methyl-4-methylphenol, gives a weak antiferromagnetic coupling constant $2J = -3.8\ cm^{-1}$ [30]. However, the dinuclear nickel (II) complexes $[Ni_2(L^2)(OPr)(H_2O)_2](ClO_4).H_2O$ and $[Ni_2(L^2)(OAc)(H_2O)][(ClO_4)_2$, where L^2 is the ligand *N*,*N*,*N*′,*N*′-tetrakis[(1-ethyl-2-benzimidazolyl)methyl]-2-hydroxy-1,3-diaminopropane, reported by Nakao and co-workers, show a relatively stronger antiferromagnetic interaction $2J = -34.4\ cm^{-1}$ and $2J = -43.2\ cm^{-1}$, respectively [31]. These authors have suggested that the basal plane around each Ni(II) is planar and the alkoxo oxygen of the ligand and the oxygen atoms from the acetate or the propionate groups bridge the two coordination planes resulting in their coplanarity.

Thus, as complex **1** shows three bridges between the nickel atoms, the Ni···Ni distance and the Ni-(Ophenolate)$_2$–Ni angles are reduced, causing a weak antiferromagnetic interaction between the nickel centers. Furthermore, the presence of an additional acetate bridge seems to reduce the extent of the exchange coupling, as suggested in the case of the diiron complexes obtained with the ligand H_2BPClNOL [13].

3.5. Mass spectrometric characterization of *1*

ESI-MS/MS has been shown to be a powerful tool for the characterization of cationic organometallic and coordination compounds in solution, even the most weakly bound ones, and we have used this technique extensively to characterize a variety of such complexes [32]. Fig. 4 shows the ESI-MS spectrum in water:methanol (1:1) solution of **1** whereas Scheme 1 summarizes the structural assignments of the detected cationic complexes. The intact cationic complex $\mathbf{1}^+$ and its characteristic set of isotopologue ions, due mainly to the presence of Ni and Cl atoms, are clearly detected. Note the mono-isotopic ion of *m*/*z* 785, the principal ion of *m*/*z* 787 as well as an abundant isotopologue ion of *m*/*z* 789. Interestingly, we also observed in Fig. 4 the ESI-MS detection of a cation containing a perchlorate group coordinated to the dinuclear unit, as a result of substitution of the acetate bridge in $\mathbf{1}^+$ by a perchlorate anion in solution. The perchlorate anion could be acting as a bridging group (principal ion of *m*/*z* 827). Recently, McKenzie and co-workers reported the X-ray crystal structure of a perchlorate-bridged dimanganese compound $[Mn_2(bpbp)(ClO_4)(H_2O)_2](ClO_4)_2$. H_2O

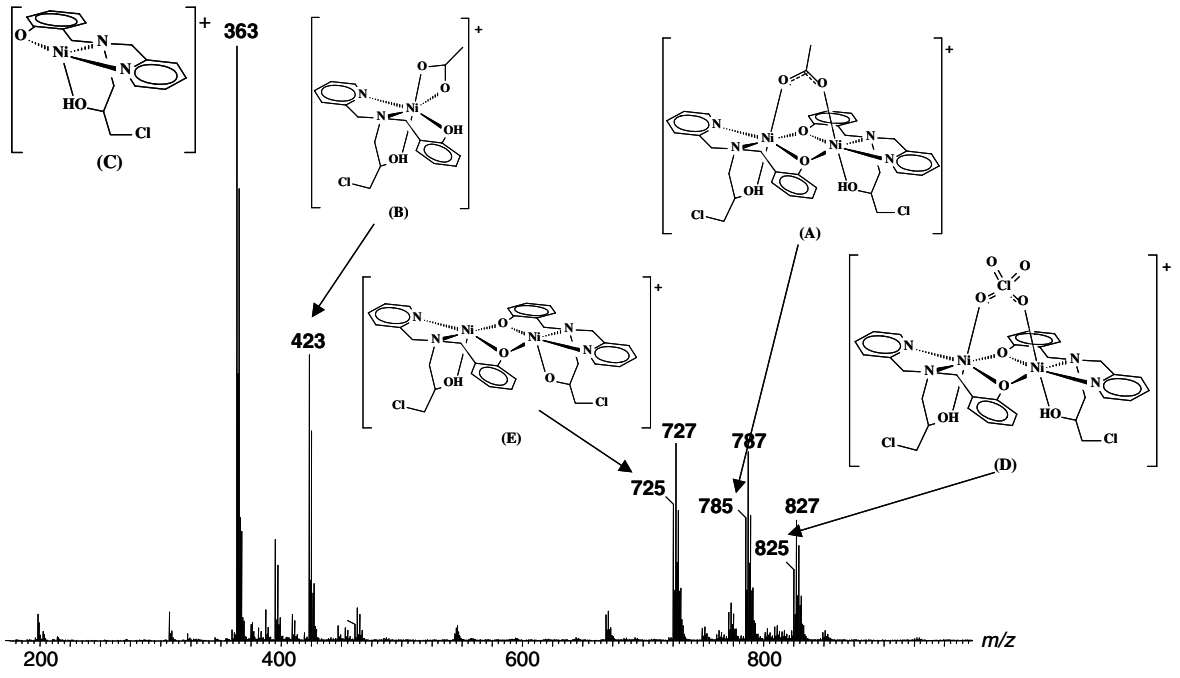

Fig. 4. ESI-MS in the positive ion mode for a water:methanol 1:1 solution of complex **1**.

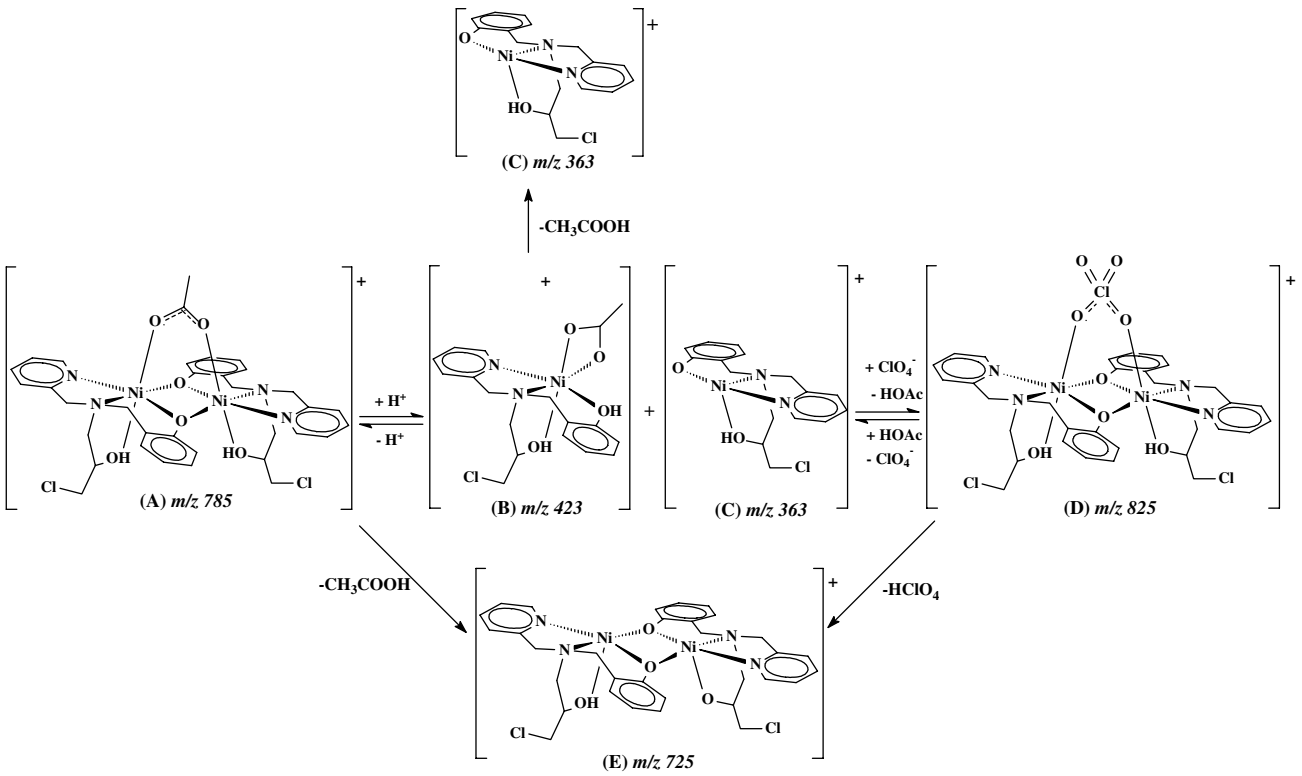

Scheme 1. Structures present in MeOH:H_2O (1:1) solution and fragments observed via ESI-MS and ESI-MS/MS experiments for complex **1**. (A), (B) and (D) are compounds present in solution. (C) and (E) are fragments observed after ionization.

(Hbpbp = 2,6-bis(*N*,*N*′-bis(2-picolyl)amino)-methyl)-4-tert-butylphenol. ESI-MS revealed that the perchlorate anion remains bound to the manganese centers in a nitromethane solution [33].

ESI-MS/MS of these ions (Fig. 5) reveals dissociations that are consistent with their structural assignments presented in Scheme 1. For instance, the tandem mass spectrum for the ion of *m*/*z* 825 (Scheme 1) shows that it dissociates mainly by the formal loss of a neutral molecule of perchloric acid of 100 Da. In fact, formal loss of $HClO_4$ occurs likely first by the loss of ClO_4^- ion, which creates an unstable doubly charged cation, which then promptly eliminates a hydrogen ion to reduce its charge state to form the singly charged fragment ion of *m*/*z* 725 (Scheme 1). Similarly, $\mathbf{1}^+$ eliminates formally a neutral molecule of acetic acid to form the same fragment ion of *m*/*z* 725 (Scheme 1 and Fig. 5b). The ESI-MS/MS of the ion of *m*/*z* 363 is also structurally characteristic; the ion loses an HCl molecule to form the fragment ion of the *m*/*z* 327 and then a neutral molecule of 106 Da to form the major fragment ion of 221 (Fig. 5c).

Due to an equilibrium in solution, the dinuclear complex $\mathbf{1}^+$ dissociates to form mononuclear compounds (Scheme 1, compounds (B) and (C)), being the mononuclear nickel (II) cation of *m*/*z* 423 unambiguously detected from solution. This conclusion is based on the fact that we have not observed the formation of this ion of *m*/*z* 423 in the ESI-MS/MS of the ions with higher *m*/*z*, that is, those of *m*/*z* 825, *m*/*z* 785 and *m*/*z* 725. Thus, our ESI-MS data indicate the presence of three cations in MeOH:H_2O (1:1) solution: $[Ni(H_2BPClNOL)(OAc)]^+$, $[Ni_2(HBPClNOL)_2(OAc)]^+$ and $[Ni_2(HBPClNOL)_2\ (ClO_4)]^+$ (Scheme 1, compounds (B), (A) and (D), respectively). Ion (C) of *m*/*z* 363 is also likely present in solution but its formation in the gas phase due to in-source dissociation cannot be entirely dismissed since the ion (B) of *m*/*z* 423, as indicated by its ESI-MS/MS, forms (C) upon collisions by the loss of a neutral molecule of acetic acid (60 Da). The ion of *m*/*z* 363 (formed in solution by dissociation of complex **1**) could react with the perchlorate ion, resulting in the dinuclear ion of *m*/*z* 825 (Scheme 1).

Dissociation of the monoisotopic of *m*/*z* 725 (E) forms a series of fragment ions mainly of *m*/*z* 653, 583, 547, 327, and 221. Although a complete dissociation scheme for this ion would require an extensive MS/MS investigation, two ions are easily characterized: that of *m*/*z* 653 is formed by the consecutive losses of two HCl molecules, whereas that of *m*/*z* 327 corresponds to the ion of *m*/*z* 363 (Scheme 1) minus an HCl molecule.

3.6. Potentiometric titration

The X-ray crystal structure for complex **1** presented in Fig. 1 reveals the absence of water molecules coordinated to the nickel center. Thus, potentiometric titration studies were performed on complex **1** in order to evaluate whether water molecules would be coordinated to the nickel ions in ethanol/water solution. The displacement of the acetate

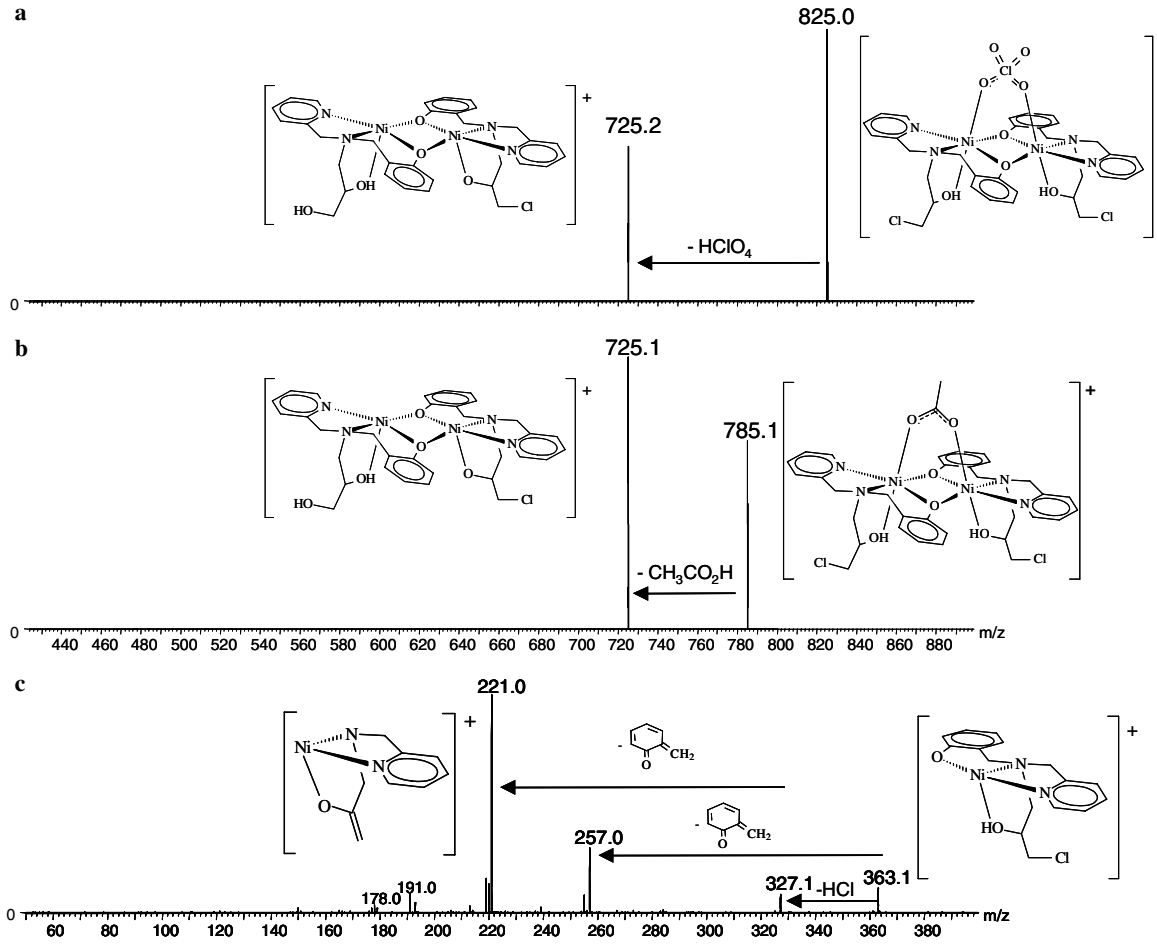

Fig. 5. ESI-MS/MS for the ions of (a) *m/z* 825.0, (b) *m/z* 785.1 and (c) *m/z* 363.1.

group by water molecules in the diiron complex $[Fe_2(BPClNOL)_2(OAc)]^+$ has been reported previously, being this iron complex obtained with the same ligand $H_2BPClNOL$. The recrystallization of the complex $[Fe_2(BPClNOL)_2(OAc)]^+$ in methanol/water resulted in the formation of the diaquo complex $[Fe(BPClNOL)_2(H_2O)_2]^+$, which was characterized by X-ray diffraction [13].

The potentiometric titration was carried out by the addition of HCl solution up to pH 3.4, followed by the addition of KOH solution. The titration curve shows two buffered regions, one below pH 8 and other above pH 8. The buffered region below pH 8 can be attributed to the equilibriums involving $HOAc/OAc^-$ and phenol/phenolate. The presence of this buffered region below pH 8 suggests that the dinuclear unit could be broken under acidic/neutral pH conditions, resulting in mononuclear compounds. This proposal is in agreement with the ESI-MS analysis, which shows that the mononuclear ion $[Ni(H_2BPClNOL)(OAc)]^+$ ($m/z = 423$) is in equilibrium with the dinuclear $[Ni_2(HBPClNOL)_2(OAc)]^+$ and $[Ni_2(HBPClNOL)_2\ (ClO_4)]^+$ ions, in solution.

Thus, at acid pH, the acetate and the phenolate groups are protonated (pK_a values of 4.98, 5.35, and 6.12, respectively), resulting in the rupture of the dinuclear unit presented in the complex **1** (Scheme 2, compound (F)). At pH 4.98 an equilibrium involving $HOAc/OAc^-$ species was observed. The presence of OAc^- ion results in the formation of the mononuclear compound containing acetate coordinated (Scheme 2, compound (G)). As the initial complex **1** has one acetate and two nickel ions, the mononuclear compound $[Ni(H_2BPClNOL)(H_2O)_2]$ (F) should also coexist in solution with the compound (G). Under the conditions employed in the potentiometric study, water molecules are also coordinated to the nickel ions, keeping the nickel ion hexacoordinated, since protonation/deprotonation equilibriums consistent with aquo/hydroxo species were observed at higher pH values.

Protonation/deprotonation equilibriums involving the phenol groups are observed at pH 5.35 and 6.12 (Fig. 6). The presence of two distinct pK_a values indicates also that two different mononuclear compounds are present in solution ((F) and (G)). The first phenol deprotonation ($pK_a = 5.35$) results in the dinuclear monobridged compound $[Ni_2(HBPClNOL)(H_2BPClNOL)(H_2O)_3]^{2+}$ (H). The second deprotonation results in the dinuclear dibridged unit $[Ni_2(HBPClNOL)_2(H_2O)_2]^{2+}$ (Scheme 2, compound (I)), which is the predominant species in the pH range from 6.12 to 9.68. The first deprotonation/protonation

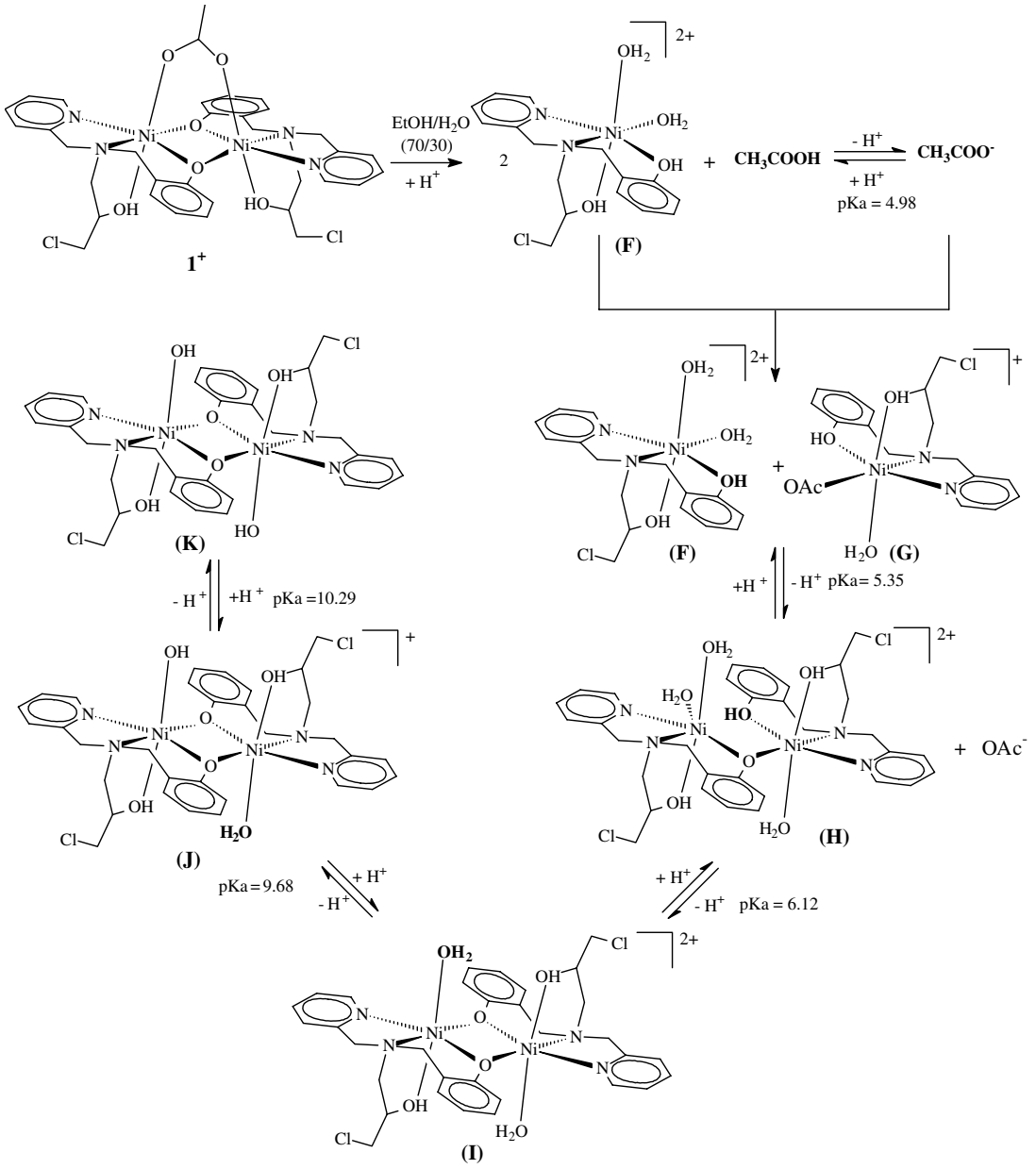

Scheme 2. Proposal of chemical species present in EtOH:H_2O (70:30) solution at different pH.

equilibrium involving the water molecules was observed at pH 9.68 (Scheme 2, compound (J)). Above this pH the aquo/hydroxo ion becomes predominant, reaching a maximum of 50% at pH 10.2. Another pK_a found at 10.29 can be attributed to the deprotonation/protonation equilibrium of the second water molecule, which leads to the dihydroxo form $[Ni_2(HBPClNOL)_2(OH)_2]$, (Scheme 2, compound (K)).

On comparing the pK_a values observed for the water molecules coordinated to nickel (II) ions in complex **1** with those measured for the water molecules coordinated to the iron(III) ions presented in the complex $[Fe_2(BPClNOL)(H_2O_2)]^+$(p$K_{a1} = 5.00$; p$K_{a2} = 7.03$) [13], it is possible to confirm the higher Lewis acidity of the iron(III) ion.

Thus, the presence of water molecules coordinated to the metal centers in complex **1**, under basic conditions, could be confirmed, and render complex **1** an interesting model for urease.

4. Conclusion

In this paper, we have reported the synthesis and characterization of a new nickel complex, which was obtained by the reaction between the ligand $H_2BPClNOL$, $[Ni(OH_2)_6](ClO_4)_2$ and sodium acetate. Complex **1**, described and characterized herein, provides some important features relevant to the search of synthetic models for urease. These features involve a distinct behavior in solid state and in solution. According to the ESI-MS experi-

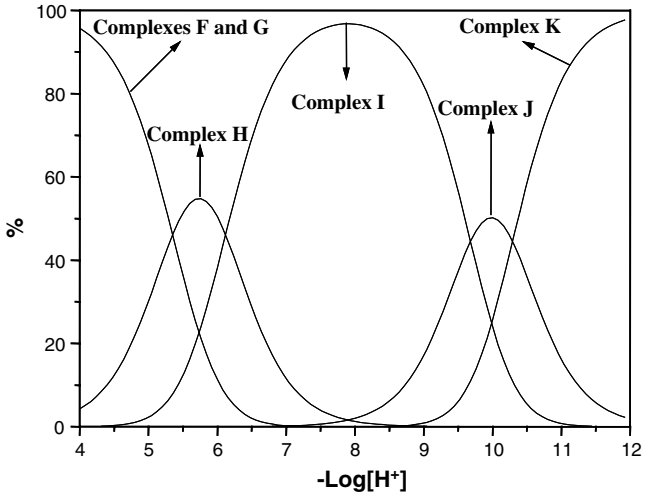

Fig. 6. Relative concentrations of mononuclear and dinuclear complexes, as a function of pH, calculated from potentiometric titration data. Complex $\mathbf{1}^{+}$: $[Ni_2(HBPClNOL)_2(OAc)]^{+}$; complex (F): $[Ni(H_2BPClNOL)(H_2O)_2]^{2+}$; complex (G): $[Ni(H_2BPClNOL)(OAc)(H_2O)]^{+}$; complex (H): $[Ni_2(HBPClNOL)(H_2BPClNOL)(H_2O)_3]^{2+}$; complex (I): $[Ni_2(HBPClNOL)_2(H_2O)_2]^{2+}$; complex (J): $[Ni_2(HBPClNOL)_2(H_2O)(OH)]^{+}$; complex (K): $[Ni_2(HBPClNOL)_2(OH)_2]$.

ments, complex **1** is in equilibrium with the mononuclear $[Ni(H_2BPClNOL)(OAc)]^{+}$ (**B**) and dinuclear $[Ni_2(HBPClNOL)_2(ClO_4)]^{+}$ (**D**) compounds, in a MeOH:H_2O (1:1) solution. Also, the potentiometric studies carried out in ethanol/water solution (70:30) support that under acid pH, complex **1** can form a mononuclear complex (**F**) by the protonation of the acetate and phenolate bridges. Above pH 6.12, the dinuclear unit is predominant. Under these conditions complex **1** becomes in fact a diaquo complex $[Ni_2(HBPCNOL)_2(H_2O)_2]^{2+}$. Above pH 9.68, the complex $[Ni_2(HBPCNOL)_2(H_2O)(OH)]^{+}$ is present in significant quantities. Thus, the formation of the aquo/hydroxo complex in solution is very interesting since the presence of water and hydroxo groups coordinated to the nickel atoms has been considered essential for the catalytic activity of urease.

5. Supplementary material

The crystallographic data (atomic coordinates and equivalent isotropic displacement parameters, calculated hydrogen atom parameters, anisotropic thermal parameters and bond lengths and angles) have been deposited at the Cambridge Crystallographic Data Center (deposition number CCDC 276647). Copies of this information may be obtained free of charge from: CCDC, 12 Union Road, Cambridge, CB2 1EZ, UK (Fax: +44 1223 336 033; e-mail: deposit@ccdc.cam.ac.uk or http://www.ccdc.cam.ac.uk).

Acknowledgements

A.H. Jr, C.F., and L.F. acknowledge the assistance of Instituto de Química- Universidade Federal do Rio de Janeiro and are grateful for grants from FAPERJ, CNPq, PRONEX and to CCDC by the free of charge License of Access to the following programs: CSD System [34], ConQuest [35], IsoStar [36]. A.J.B. is grateful to FINEP. M.A.N. is grateful to FAPERJ, CAPES, CNPq, FUJB and Instituto do Milênio de Nanociências. M.B.N., L.S.E., R.R.C., and M.N.E. are grateful for grants from FAPESP and CNPq. The authors are grateful to M.G.F. Vaz (Univ. Fed. Fluminense) for the fit of the magnetic data.

References

[1] S. Ciurli, S. Benini, W.R. Rypniewski, K.S. Wilson, S. Miletti, S. Managni, Coord. Chem. Rev. 190–192 (1999) 331.
[2] A.M. Barrios, S.J. Lippard, J. Am. Chem. Soc. 122 (2000) 9172.
[3] J.B. Summer, J. Biol. Chem. 69 (1926) 435.
[4] E. Jabri, M.B. Carr, R.P. Hausinger, P.A. Karplus, Science 268 (1995) 998.
[5] P.A. Clark, D.E. Wilkox, Inorg. Chem. 28 (1989) 1326.
[6] K.P. Day, J. Peterson, M.S. Sendova, M.J. Todd, R.P. Hausinger, Inorg. Chem. 32 (1993) 634.
[7] M.G. Finnegan, A.T. Kowal, M.T. Werth, P.A. Clark, D.E. Wilkox, M.K. Johnson, J. Am. Chem. Soc. 113 (1991) 4030.
[8] R.L. Blakeley, A. Treston, R.K. Andrews, B. Zenner, J. Am. Chem. Soc. 104 (1982) 612.
[9] H.L.T. Mobley, M.D. Island, R.P. Hausinger, Microbiol. Rev. 59 (1995) 451.
[10] S. Benini, W.R. Rypniewski, K.S. Wilson, S. Miletti, S. Ciurli, S. Mangani, Structure 7 (1999) 205.
[11] S. Benini, W.R. Rypniewski, K.S. Wilson, S. Miletti, S. Ciurli, S. Managni, J. Biol. Inorg. Chem. 5 (2000) 110.
[12] (a) P. Chaudhuri, H.-J. Küppers, K. Wiegkardt, S. Gehring, W. Haase, B. Nuber, J. Weiss, J. Chem. Soc., Dalton Trans. (1988) 1367;
(b) D. Volkmer, A. Hörstmann, K. Griesar, W. Haase, B. Krebs, Inorg. Chem. 35 (1996) 1132;
(c) F. Meyer, E. Kaifer, P. Kircher, K. Heinze, H. Pritzkow, Chem. Eur. J. (1999) 1617;
(d) A.M. Barrios, S.J. Lippard, Inorg. Chem. 40 (2001) 1250;
(e) A.J. Stemmler, J.W. Kampf, M.L. Kirk, V.L. Pecoraro, J. Am. Chem. Soc. 117 (1995) 6368;
(f) S. Uozumi, H. Furtachi, M. Obba, H. Okaza, D.E. Fenton, K. Shindo, S. Murata, D.J. Kitko, Inorg. Chem. 37 (1998) 6281;
(g) K. Yamaguchi, S. Koshino, M. Suzuki, A. Uehara, S. Suzuki, J. Inorg. Biochem. 67 (1997) 187;
(h) K. Yamaguchi, S. Koshino, F. Akagi, M. Suzuki, A. Uehara S. Suzuki, J. Am. Chem. Soc. 119 (1997) 5752;
(i) A.M. Barrios, S.J. Lippard, J. Am. Chem. Soc. 121 (1999) 11751;
(j) S. Buchler, F. Meyer, E. Kaifer, H. Pritzkow, Inorg. Chim. Acta 337 (2002) 371;
(k) K. Rudza, A.M. Arif, L.M. Berreau, Inorg. Chem. 44 (2005) 7234;
(l) H. Carlsson, M. Haukka, E. Nordlander, Inorg. Chem. 41 (2001) 4981;
(m) D.A. Brown, W.K. Glass, N.J. Fitzpatrick, T.J. Kemp, W. Errington, H. Müller-Bunz, A.J. Hussein, H. Nimir, Inorg. Chim. Acta 358 (2005) 2755.
[13] A. Horn Jr., I. Vencato, A.J. Bortoluzzi, R. Hörner, R.A.N. Silva, B. Szpoganicz, V. Drago, H. Terenzi, M.C.B. De Oliveira, R. Werner, W. Haase, A. Neves, Inorg. Chim. Acta 358 (2005) 339.
[14] A.E. Martell, R.J. Motekaitis, Determination and Use of Stability Constants, second ed., VHC Publishers, 1992.
[15] A. Neves, M.A. de Brito, I. Vencato, V. Drago, K. Griesar W. Haase, Y.P. Mascarenhas, Inorg. Chim. Acta 214 (1993) 5.
[16] A. Horn Jr., A. Neves, I. Vencato, V. Drago, C. Zucco, R. Werner, W. Haase, J. Braz. Chem. Soc. 11 (2000) 7.

[17] W.J. Geary, Coord. Chem. Rev. 7 (1971) 81.
[18] A.L. Spek, HELENA; CAD-4 Data Reduction Program, University of Utrecht, The Netherlands, 1996.
[19] (a) A.L. Spek, PLATON; Molecular Geometry and Plotting Program, University of Utrecht, The Netherlands, 1997;
(b) A.C.T. North, D.C. Phillips, F.S. Mathews, Acta Crystallogr. A 24 (1968) 351.
[20] A. Altomare, M.C. Burla, M. Camalli, G. Cascarano, C. Giacovazzo, A. Guagliard, A.G.G. Moliterni, R. Spagna, J. Appl. Cryst. 32 (1999) 115.
[21] G.M. Sheldrick, SHELXL97. Program for the Refinement of Crystal Structures, University of Göttingen, Germany, 1997.
[22] L.J. Farrugia, J. Appl. Cryst., C 39 (1983) 565.
[23] K. Nakamoto, Infrared and Raman Spectra of Inorganic and Coordination Compounds, Wiley, New York, 1978.
[24] A. Greatti, M.A. de Brito, A.J. Bortoluzzi, A.S. Ceccato, J. Mol. Struct. 688 (2004) 185.
[25] M.A. Brito, A.J. Bortoluzzi, A. Greatti, A.S. Ceccato, A.C. Joussef, S.M. Drechsel, Acta Cryst. Sect. C 56 (2000) 1188.
[26] T.R. Holman, M.P. Hendrich, L. Que Jr., Inorg. Chem. 31 (1992) 939.
[27] R.L. Blakeley, N.E. Dixon, B. Zerner, Biochim. Biophys. Acta 744 (1983) 219.
[28] D. Volkmer, A. Hörstmann, K. Griesar, W. Haase, B. Krebs, Inorg. Chem. 35 (1996) 1132.
[29] S.K. Dey, N. Mondal, S.E. Fallah, R. Vincete, A. Escuer, X. Solans, M. Font-Bardía, T. Matsushita, V. Gramlich, S. Mitra, Inorg. Chem. 43 (2004) 2427.
[30] R.M. Buchanan, M.S. Mashuta, K.J. Oberhausen, J.F. Richardson, J. Am. Chem. Soc. 111 (1989) 4497.
[31] Y. Hosokawa, H. Yamane, Y. Nakao, K. Matsumoto, S. Takamizawa, W. Mori, S. Suzuki, H. Kimoto, Inorg. Chim. Acta 283 (1998) 118.
[32] (a) H.E. Toma, A.D.P. Alexiou, A.L.B. Formiga, M. Nakamura, S. Dovidauskas, M.N. Eberlin, D.M. Tomazela, Inorg. Chim. Acta 358 (2005) 2891;
(b) R.M.S. Pereira, V.I. Paula, R. Buffon, D.M. Tomazela, M.N. Eberlin, Inorg. Chim. Acta 357 (2004) 2100;
(c) I. Mayer, M.N. Eberlin, D.M. Tomazela, H.E. Toma, K. Araki, J. Braz. Chem. Soc. 16 (2005) 418;
(d) G. Cerchiaro, P.L. Saboya, A.M. da Costa Ferreira, D.M. Tomazela, M.N. Eberlin, Transition Met. Chem. 29 (2004) 495;
(e) I. Mayer, A.L.B. Formiga, F.M. Engelmann, H. Winnischofer, P.V. Oliveira, D.M. Tomazela, M.N. Eberlin, H.E. Toma, K. Araki, Inorg. Chim. Acta 358 (2005) 2629;
(f) D.M. Tomazela, I. Mayer, F.M. Engelmann, K. Araki, H.E. Toma, M.N. Eberlin, J. Mass Spectrom. 39 (2004) 1161;
(g) G.T.S. Martins, B. Szpoganicz, V. Tomisic, N. Humbert, M. Elhabiri, A. Albrecht-Gary, L.F. Sala, Inorg. Chim. Acta 357 (2004) 2261–2268.
[33] K.B. Jensen, E. Johansen, F.B. Laresen, C.J. McKenzie, Inorg. Chem. Commun. 43 (2004) 3801.
[34] F.H. Aleen, Acta Cryst., B 58 (2002) 380.
[35] I.J. Bruno, J.C. Cole, P.R. Edington, M. Kessler, C.F. Macrae, P. McCabe, J. Pearson, R. Taylor, Acta Cryst. B 58 (2002) 389.
[36] I.J. Bruno, J.C. Cole, J.P.M. Lommerse, R.S. Rowland, R. Taylor, M. Verdonl, J. Comput. Aided Mol. Des. 11 (1997) 525.